Systematic study of the isotopic dependence of fusion dynamics for neutron- and proton-rich nuclei using a proximity formalism

O. N. Ghodsi, R. Gharaei,* and F. Lari

Sciences Faculty, Department of Physics, University of Mazandaran P. O. Box 47415-416, Babolsar, Iran

(Received 8 May 2012; revised manuscript received 14 July 2012; published 31 August 2012)

The behaviors of barrier characteristics and fusion cross sections are analyzed by changing neutrons over a wide range of colliding systems. For this purpose, we have extended our previous study [Ghodsi and Gharaei, Eur. Phys. J. A **48**, 21 (2012), it is devoted to the colliding systems with neutron-rich nuclei] to 125 isotopic systems with the condition of $0.5 \leqslant N/Z \leqslant 1.6$ for their compound nuclei. The AW 95, Bass 80, Denisov DP, and Prox. 2010 potentials are used to calculate the nuclear part of the interacting potential. The obtained results show that the trend of barrier heights V_B and positions R_B as well as nuclear V_N and Coulomb V_C potentials (at $R = R_B$) as a function of $(N/Z - 1)$ quantity are nonlinear (second order) whereas the fusion cross sections follow a linear dependence.

DOI: 10.1103/PhysRevC.86.024615 PACS number(s): 24.10.−i, 25.60.Pj, 25.70.Jj

I. INTRODUCTION

The systematic study of the isotopic dependence of the interacting potential and fusion cross sections is one of the interesting subjects in nuclear physics. It is carried out using different theoretical models such as the Skyrme energy density formalism, Ngô and Ngô, Christensen and Winther, and the Bass and Denisov potentials [1–3], although, the choice of these potentials was not made on merit to reproduce the experimental data. One can divide the isotopic systems in previous studies into three series: different collisions of Ca and Ni isotopes with conditions of (i) $1 \leqslant N/Z \leqslant 2$ [1], (ii) $0.6 \leqslant N/Z \leqslant 2$ [2], and (iii) $0.5 \leqslant N/Z \leqslant 2$ [3]. In these conditions N and Z are the neutron and proton numbers of a compound nucleus. In all mentioned investigations, the isotopic dependence of barrier heights V_B and positions R_B as well as fusion cross sections σ_{fus} versus the N/Z ratio have been examined. The obtained results show that the increasing trend of R_B and σ_{fus} and the decreasing trend of V_B as a function of the N/Z ratio for fusion systems with condition (i) are linear, see Fig. 2 of Ref. [1]. However, in different collisions of Ca and Ni isotopes which have a condition of $0.6 \leqslant N/Z \leqslant 2$ (or $0.5 \leqslant N/Z \leqslant 2$), it is shown that this behavior is nonlinear (second order) for R_B and V_B whereas the fusion cross sections follow a linear dependence (see the corresponding figures of Refs. [2,3]). As a result, one expects that with the increase of a neutron and its effect on the attractive force, the Coulomb barrier heights decrease. Since the fusion probability is directly dependent on these parameters, it is therefore predictable that the fusion cross sections increase with the addition of a neutron in different isotopic systems. As an important issue, it can be noted that the experimental data have only been reported for fusion reactions with nuclei which are near the stability line ($N = Z$). Therefore one can compare the measured and calculated values of fusion cross sections for limited numbers of reactions. However, using the proposed semi-empirical approaches, such as Ref. [4], the experimental data are well described.

In a recent study, we analyzed the isotopic dependence of fusion cross sections and barrier characteristics for 50 fusion reactions with a condition of $1 \leqslant N/Z \leqslant 1.6$ [5]. For this purpose, we selected the fusion reactions which the C, O, Mg, Si, S, Ca, Ar, Ti, and Ni isotopes are as their participant nuclei. In this study, the nuclear part of the interacting potential was calculated using four versions of the proximity model, namely AW 95 [6], Bass 80 [7,8], Denisov DP [9], and Prox. 2010 [10] potentials. It is shown that these models have good agreement with experimental data [10–12]. Our obtained results, like Ref. [1], confirmed the linear trend of R_B, V_B, and σ_{fus} versus N/Z ratio for fusion reactions with $1 \leqslant N/Z \leqslant 1.6$.

In the present work, we are going to extend our studies to both proton- and neutron-rich systems. For this purpose, we chose 125 fusion reactions so that all colliding pairs are assumed to be spherical and the N/Z ratio of compound nuclei, which are formed during fusion process, to be in the range $0.5 \leqslant N/Z \leqslant 1.6$. For neutron-deficient systems, we only intended to investigate the influence of the changing neutron on the input potential channel and fusion probabilities. The lightest (^{10}C) and heaviest (^{54}Ni) proton-rich nuclei have the half-life $T_{1/2} = 19.30$ s and $T_{1/2} = 104.00$ ms, respectively. The proximity formalism and Wong model [13] are employed to calculate the nuclear potentials and fusion cross sections, respectively.

In summary, our motivations in this work are as follows. (i) There is no systematic study on the isotopic dependence of fusion cross sections based on the AW 95, Bass 80, Denisov, and Prox. 2010 potentials in the range of $N/Z \leqslant 1$. The applied models in previous studies [1–3] were not made on merit to reproduce the experimental data whereas our selected models are able to reproduce experimental data within 10%, on the average, see Refs. [10–13] for details. (ii) The different colliding systems in previous work [1–3] are only the included Ca and Ni isotopes whereas, we used the C, O, Mg, Si, S, Ca, Ar, Ti, and Ni nuclei as colliding pairs that have been taken from the proton-rich region of periodic table. Our selections can be more appropriate fo ar better understanding of the isotopic dependence of R_B, V_B, and σ_{fus} versus the N/Z ratio. (iii) The isotopic systems that were used in previous studies

*r.gharaei@stu.umz.ac.ir

such as Refs. [1–3] lie far from the stability line ($N = Z$) and in these regions the experimental data have not been reported. Whereas, using the present study, one can analyze the calculated results and compare them with the corresponding experimental data. (iv) Such studies can be very useful to predict the properties of new and superheavy elements that are produced in the fusion process and are not available at present.

The study of neutron-rich nuclei is also reported at heavy-ion collisions with intermediate energies. The effects of the isospin degree of freedom in collective and elliptic flow have been studied, for example, by the authors of Refs. [14–17]. Recently, using the dynamic approach based on the macroscopic models, the isospin effects have been examined for ^{40}Ca + ^{90,96}Zr, ^{48}Ca + ^{90}Zr fusion reactions [18]. The obtained results reveal that the dynamic effects decrease barrier height and thickness.

The paper is organized as follows. In Sec. II, we discuss the nuclear part of the total interaction potential as well as the employed models for calculating it. The analysis of the isotopic dependence of barrier characteristics and fusion cross sections in different ranges of the N/Z ratio have been carried out in Secs. III and IV. Section V is devoted to some concluding remarks.

II. THE NUCLEAR POTENTIAL OF INTERACTING SYSTEMS

In general, with the assumption that the participant nuclei in a fusion reaction to be in the s-wave state ($\ell = 0$), the total potential can be defined as the sum of two parts which are caused by electrostatic (Coulomb-repulsion) and strong (nuclear-attraction) interactions. In recent years, many theoretical models have been introduced to parametrize the last interactions. The proximity formalism is one of the useful models for the calculating of the nuclear potential. The various versions of this formalism are introduced in Refs. [10–12]. These studies were carried out on many different systems. The obtained results show that all introduced models determine the fusion barrier heights with an accuracy of ±10%, on the average. Among various versions, our selected potentials, namely AW 95, Bass 80, Denisov DP, and Prox. 2010, reproduce the best results for potential and fusion cross sections. These models are briefly explained in the following.

Winther proposed a nuclear potential which is parameterized based on the Woods-Saxon form [6]

$$V_N^{\mathrm{AW95}}(r) = -\frac{V_0}{1+\exp\left(\frac{r-R_0}{a}\right)}, \tag{1}$$

here the V_0, R_0, and a parameters are defined as

$$V_0 = 16\pi\frac{R_1R_2}{R_1+R_2}\gamma a, \tag{2}$$

$$R_0 = R_1 + R_2, \tag{3}$$

and

$$a = \left[\frac{1}{1.17\left(1+0.53\left(A_1^{-1/3}+A_2^{-1/3}\right)\right)}\right]. \tag{4}$$

The R_i and γ parameters in Eqs. (2) and (3), respectively, stand for the radius of the target/projectile and surface energy coefficient and can be written as

$$R_i = 1.2A_i^{1/3} - 0.09\ (i=1,2), \tag{5}$$

$$\gamma = 0.95\left[1 - 1.8\left(\frac{N_p - Z_p}{A_p}\right)\left(\frac{N_t - Z_t}{A_t}\right)\right], \tag{6}$$

where $A_{p(t)}$, $Z_{p(t)}$, and $N_{p(t)}$ are characteristics of the target and projectile.

According to the proximity theorem [19], the nuclear potentials that are based on the models such as Bass 80, Denisov, and Porx. 2010 are defined as the product of a geometrical factor and a universal function which are, respectively, dependent on the mean curvature of the interaction surface and the separation distance. Therefore one can use the below equations to calculate the nuclear potential based on the selected models

$$V_N^{\mathrm{Bass80}}(r) = -\frac{R_1R_2}{R_1+R_2}\Phi(s = r - R_1 - R_2), \tag{7}$$

$$V_N^{\mathrm{DenisovDP}}(r) = -1.989843\frac{R_1R_2}{R_1+R_2}\Phi(s = r - R_1 - R_2 - 2.65) \times\left[1 + 0.003525139\left(\frac{A_1}{A_2}+\frac{A_2}{A_1}\right)^{3/2} - 0.4113263(I_1+I_2)\right], \tag{8}$$

$$V_N^{\mathrm{Prox.2010}}(r) = 4\pi\gamma\frac{R_1R_2}{R_1+R_2}\Phi(s = r - C_1 - C_2). \tag{9}$$

In these relations the radius parameter R_i can be written as follows:

$$R_i^{\mathrm{Bass80}} = R_s\left(1 - \frac{0.98}{R_s^2}\right), \quad (i=1,2), \tag{10}$$

$$R_i^{\mathrm{Denisov}DP} = 1.2332A_i^{1/3}(1 + 2.348443/A_i - 0.151541A_{si}), \quad (i=1,2), \tag{11}$$

where the sharp radius R_s in Eq. (10) is given as $R_s = 1.28A^{1/3} - 0.76 + 0.8A^{-1/3}$. The R_i parameter in Prox. 2010 is similar to the AW 95 model, Eq. (5). The universal function $\Phi(s)$ is, respectively, defined by Eqs. (20), (42), and (6) of Ref. [11] for Bass 80, Denisov DP, and Prox. 2010 potentials.

III. ISOTOPIC ANALYSIS OF TOTAL POTENTIALS

By adding the Coulomb part to our selected nuclear potentials, which are introduced in previous sections, one can calculate the total interaction potential for different fusion systems by following the simple expression

$$V_{\text{tot}}(r) = V_N(r) + V_C(r) = V_N(r) + \frac{Z_1 Z_2 e^2}{r}, \qquad (12)$$

where Z_1 and Z_2 are atomic numbers of interaction nuclei. The effects of the addition/removal of a neutron on the various potentials are shown in Fig. 1. In this figure, the nuclear $V_N(r)$, Coulomb $V_C(r)$, and total $V_T(r)$ potentials are separately plotted for ^{A_1}Ni+^{A_2}Ni isotopic systems, which consist of proton-rich (^{48}Ni + ^{48}Ni, ^{50}Ni + ^{50}Ni and ^{54}Ni + ^{54}Ni), neutron-rich (^{58}Ni + ^{58}Ni and ^{64}Ni + ^{64}Ni), as well as symmetric (^{56}Ni + ^{56}Ni) participant nuclei. Using the results shown in Fig. 1, the influence of neutron excess on the shape of the considered potentials is quite evident.

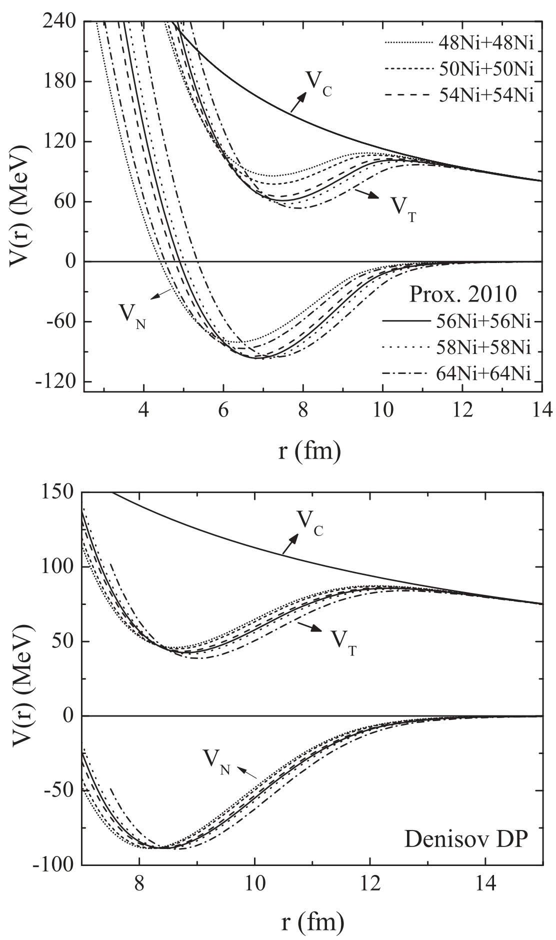

FIG. 1. The various components of the interacting potential (i.e., nuclear V_N, Coulomb V_C, and total V_T potentials) versus internuclear distance r (in fm) for the ^{A_1}Ni + ^{A_2}Ni isotopic system. These calculations are based on the Prox. 2010 and Denisov DP potentials, for example.

The exact values of the barrier height V_B^{theor} and barrier position R_B^{theor} were extracted using

$$\left(\frac{dV_{\text{tot}}(r)}{dr}\right)_{r=R_B^{\text{theor}}} = 0; \quad \left(\frac{d^2V_{\text{tot}}(r)}{dr^2}\right)_{r=R_B^{\text{theor}}} \leqslant 0. \qquad (13)$$

In the beginning, we calculated the barrier heights and positions for different fusion systems using four types of proximity potentials, namely AW 95, Bass 80, Denisov DP, and Prox. 2010. The obtained results of these calculations are listed in Table I. It can be seen that with the addition of a neutron in the interacting systems the barrier heights and positions, respectively, decrease and increase. Moreover, using the definition of the Coulomb potential $V_C(r) = Z_1 Z_2 e^2/r$, we expect that by increasing R_B in any isotopic system the values of $V_C(r = R_B)$ reduce.

To get a better comparison between the experimental and theoretical values of barrier heights and positions, we displayed the V_B^{theor} versus V_B^{exp} and the R_B^{theor} versus R_B^{exp}, see Figs. 2 and 3. It is shown that the calculated values of V_B^{theor} based on the considered models have good compatibility with the experimental data. However, according to Fig. 3, one cannot find a regular behavior in predictions of barrier positions. This may be caused by the large uncertainties of these values.

A. The isotopic dependence of barrier heights V_B and positions R_B

The percentage difference of barrier characteristics [i.e., $\Delta R_B(\%)$ and $\Delta V_B(\%)$] are defined as follows to study the isotopic dependence of barrier heights and positions:

$$\Delta R_B(\%) = \frac{R_B - R_B^0}{R_B^0} \times 100, \qquad (14)$$

$$\Delta V_B(\%) = \frac{V_B - V_B^0}{V_B^0} \times 100. \qquad (15)$$

Above, R_B^0 and V_B^0 are the barrier characteristics of the $N = Z$ case. Indeed, using the proposed producer of Refs. [1–3], our criterion to analyze the trend of R_B and V_B versus the N/Z ratio in each set of colliding systems is the symmetric reaction of that set. Using the straight-line interpolation between known values, we estimated the barrier characteristics (R_B and V_B) for symmetric reactions ($N = Z$) that these values are not available for them. The obtained results for Eqs. (14) and (15) based on the selected proximity potentials are plotted in Fig. 4. It is clear that with the addition of neutron, the values of R_B and V_B, respectively, increase and decrease. Moreover, Fig. 4 shows the regular behaviors for barrier heights and positions. One can analyze these behaviors using the following ranges of the N/Z ratio.

1. *Ranges of* $0.5 \leqslant N/Z \leqslant 1$ *and* $1 \leqslant N/Z \leqslant 1.6$

The values of barrier heights and positions based on the considered proximity potentials follow a linear dependence for

TABLE I. The obtained values for barrier positions R_B and heights V_B based on the AW 95, Bass 80, Denisov DP, and Prox. 2010 potentials for neutron-deficient and neutron-rich systems.

Reaction	N/Z	R_B[a] (fm)	V_B[a] (MeV)	R_B[b] (fm)	V_B[b] (MeV)	R_B[c] (fm)	V_B[c] (MeV)	R_B[d] (fm)	V_B[d] (MeV)
$^{10}C + ^{22}Si$	0.6	7.76	14.35	7.78	11.14	7.40	14.76	7.34	14.79
$^{12}C + ^{22}Si$	0.7	8.08	13.82	8.04	13.73	7.81	14.06	7.75	14.09
$^{12}C + ^{24}Si$	0.8	8.22	13.61	8.19	13.51	8.02	13.71	7.98	13.73
$^{12}C + ^{26}Si$	0.9	8.35	13.41	8.32	13.32	8.20	13.41	8.15	13.47
$^{12}C + ^{28}Si$	1	8.47	13.23	8.45	13.14	8.36	13.15	8.29	13.26
$^{12}C + ^{29}Si$	1.05	8.53	13.15	8.51	13.05	8.43	13.04	8.35	13.18
$^{12}C + ^{30}Si$	1.1	8.58	13.07	8.57	12.97	8.50	12.92	8.41	13.10
$^{12}O + ^{20}Mg$	0.6	7.73	16.43	7.76	16.18	7.24	17.09	7.33	16.94
$^{12}O + ^{22}Mg$	0.7	7.94	16.05	7.92	15.89	7.50	16.62	7.63	16.33
$^{12}O + ^{24}Mg$	0.8	8.12	15.72	8.07	15.64	7.70	16.23	7.85	15.92
$^{14}O + ^{24}Mg$	0.9	8.33	15.34	8.30	15.26	8.08	15.53	8.12	15.45
$^{16}O + ^{24}Mg$	1	8.52	15.02	8.50	14.93	8.37	15.01	8.34	15.08
$^{16}O + ^{26}Mg$	1.1	8.65	14.81	8.65	14.72	8.53	14.72	8.47	14.88
$^{18}O + ^{24}Mg$	1.1	8.70	14.74	8.68	14.65	8.60	14.60	8.52	14.80
$^{12}O + ^{22}Si$	0.545	7.72	19.18	7.77	18.83	7.18	20.04	7.21	20.03
$^{14}O + ^{22}Si$	0.636	8.02	18.53	8.00	18.35	7.59	19.12	7.64	19.04
$^{16}O + ^{22}Si$	0.727	8.27	18.02	8.21	17.94	7.92	18.45	7.95	18.36
$^{16}O + ^{24}Si$	0.818	8.41	17.74	8.36	17.67	8.13	18.00	8.16	17.94
$^{16}O + ^{26}Si$	0.909	8.54	17.49	8.50	17.41	8.32	17.62	8.33	17.62
$^{16}O + ^{28}Si$	1	8.66	17.26	8.63	17.18	8.48	17.29	8.46	17.36
$^{16}O + ^{29}Si$	1.045	8.72	17.15	8.69	17.07	8.56	17.14	8.52	17.25
$^{16}O + ^{30}Si$	1.090	8.77	17.05	8.75	16.96	8.63	17.00	8.58	17.15
$^{18}O + ^{28}Si$	1.090	8.83	16.94	8.81	16.86	8.72	16.82	8.64	17.03
$^{20}Mg + ^{30}S$	0.786	8.66	29.50	8.60	29.42	8.25	30.35	8.40	29.97
$^{22}Mg + ^{30}S$	0.857	8.82	29.01	8.76	28.95	8.48	29.59	8.59	29.37
$^{20}Mg + ^{32}S$	0.857	8.79	29.10	8.72	29.07	8.40	29.85	8.55	29.50
$^{22}Mg + ^{32}S$	0.928	8.94	28.65	8.88	28.60	8.63	29.12	8.73	28.96
$^{24}Mg + ^{32}S$	1	9.08	28.24	9.03	28.18	8.84	28.51	8.88	28.50
$^{24}Mg + ^{34}S$	1.071	9.18	27.94	9.14	27.88	8.98	28.10	8.99	28.20
$^{26}Mg + ^{32}S$	1.071	9.21	27.87	9.17	27.80	9.02	27.99	9.01	28.12
$^{26}Mg + ^{34}S$	1.143	9.31	27.60	9.28	27.50	9.16	27.60	9.11	27.84
$^{22}Si + ^{22}Si$	0.571	8.18	31.70	8.19	31.35	7.68	33.09	7.73	32.98
$^{22}Si + ^{24}Si$	0.643	8.37	31.06	8.34	30.85	7.90	32.26	8.01	31.94
$^{24}Si + ^{24}Si$	0.714	8.54	30.50	8.49	30.37	8.12	31.47	8.24	31.12
$^{24}Si + ^{26}Si$	0.786	8.69	30.01	8.63	29.93	8.31	30.80	8.43	30.48
$^{26}Si + ^{26}Si$	0.857	8.83	29.57	8.77	29.51	8.49	30.16	8.60	29.94
$^{26}Si + ^{28}Si$	0.928	8.97	29.17	8.91	29.12	8.66	29.61	8.75	29.48
$^{28}Si + ^{28}Si$	1	9.09	28.80	9.04	28.74	8.85	29.08	8.89	29.07
$^{28}Si + ^{30}Si$	1.071	9.20	28.46	9.16	28.40	9.00	28.61	9.01	28.72
$^{30}Si + ^{30}Si$	1.143	9.31	28.15	9.29	28.06	9.16	28.17	9.12	28.41
$^{26}Si + ^{52}Ni$	0.857	9.49	55.12	9.42	55.07	9.18	56.28	9.30	55.81
$^{26}Si + ^{54}Ni$	0.904	9.57	54.70	9.50	54.66	9.28	55.77	9.39	55.32
$^{26}Si + ^{56}Ni$	0.952	9.65	54.29	9.58	54.26	9.36	55.29	9.47	54.87
$^{28}Si + ^{52}Ni$	0.904	9.62	54.41	9.55	54.39	9.36	55.32	9.44	55.04
$^{28}Si + ^{54}Ni$	0.952	9.70	54.03	9.64	53.98	9.45	54.83	9.53	54.60
$^{28}Si + ^{58}Ni$	1.048	9.84	53.30	9.79	53.22	9.62	53.94	9.68	53.81
$^{28}Si + ^{62}Ni$	1.143	9.98	52.63	9.94	52.52	9.78	53.14	9.80	53.16
$^{28}Si + ^{64}Ni$	1.190	10.04	52.31	10.01	52.19	9.85	52.78	9.86	52.88
$^{30}Si + ^{58}Ni$	1.095	9.96	52.73	9.92	52.62	9.78	53.14	9.79	53.22
$^{30}Si + ^{62}Ni$	1.190	10.09	52.10	10.07	51.94	9.94	52.37	9.92	52.61
$^{30}Si + ^{64}Ni$	1.238	10.15	51.80	10.14	51.61	10.01	52.01	9.97	52.35
$^{34}Ca + ^{34}Ca$	0.7	9.09	58.45	9.02	57.29	8.69	60.26	8.83	59.69
$^{36}Ca + ^{36}Ca$	0.8	9.33	57.10	9.25	57.05	8.99	58.52	9.12	57.96
$^{38}Ca + ^{38}Ca$	0.9	9.54	55.94	9.47	55.92	9.26	57.01	9.36	56.60

TABLE I. (*Continued.*)

Reaction	N/Z	R_B[a] (fm)	V_B[a] (MeV)	R_B[b] (fm)	V_B[b] (MeV)	R_B[c] (fm)	V_B[c] (MeV)	R_B[d] (fm)	V_B[d] (MeV)
$^{40}Ca + ^{34}Ca$	0.85	9.44	56.50	9.35	56.53	9.10	57.87	9.24	57.30
$^{40}Ca + ^{36}Ca$	0.9	9.54	55.94	9.47	55.94	9.25	57.06	9.36	56.62
$^{40}Ca + ^{38}Ca$	0.95	9.64	55.42	9.57	55.39	9.38	56.33	9.47	56.02
$^{40}Ca + ^{40}Ca$	1	9.74	54.92	9.68	54.88	9.50	55.67	9.57	55.48
$^{40}Ca + ^{44}Ca$	1.1	9.91	54.01	9.87	53.93	9.72	54.51	9.75	54.55
$^{40}Ca + ^{48}Ca$	1.2	10.08	53.18	10.05	53.08	9.92	53.51	9.90	53.78
$^{48}Ca + ^{48}Ca$	1.4	10.38	51.75	10.42	51.40	10.33	51.52	10.18	52.40
$^{38}Ca + ^{38}Ti$	0.809	9.44	62.06	9.36	62.04	9.10	63.58	9.24	62.97
$^{38}Ca + ^{40}Ti$	0.857	9.55	61.46	9.47	61.44	9.24	62.78	9.55	61.46
$^{38}Ca + ^{42}Ti$	0.857	9.64	60.91	9.57	60.88	9.36	62.05	9.64	60.91
$^{38}Ca + ^{44}Ti$	0.952	9.73	60.38	9.67	60.36	9.47	61.38	9.57	61.02
$^{40}Ca + ^{38}Ti$	0.857	9.55	61.42	9.47	61.44	9.23	62.81	9.36	62.25
$^{40}Ca + ^{40}Ti$	0.904	9.65	60.86	9.57	60.86	9.36	62.03	9.47	61.58
$^{40}Ca + ^{42}Ti$	0.952	9.74	60.34	9.67	60.32	9.48	61.32	9.58	60.98
$^{40}Ca + ^{46}Ti$	1.048	9.91	59.37	9.86	59.30	9.70	60.07	9.76	59.95
$^{40}Ca + ^{48}Ti$	1.095	10.00	58.92	9.95	58.84	9.80	59.51	9.84	59.50
$^{40}Ca + ^{50}Ti$	1.143	10.07	58.49	10.04	58.40	9.90	59.00	9.91	59.09
$^{26}S + ^{52}Ni$	0.772	9.34	63.79	9.26	63.71	8.94	65.75	9.14	64.80
$^{26}S + ^{56}Ni$	0.863	9.52	62.71	9.43	62.75	9.13	64.56	9.34	63.55
$^{28}S + ^{52}Ni$	0.818	9.48	62.95	9.40	62.89	9.14	64.52	9.29	63.81
$^{28}S + ^{56}Ni$	0.909	9.65	61.96	9.57	61.96	9.32	63.38	9.48	62.68
$^{30}S + ^{52}Ni$	0.863	9.61	62.18	9.54	62.15	9.31	63.46	9.43	62.94
$^{30}S + ^{56}Ni$	0.954	9.77	61.27	9.70	61.24	9.50	62.36	9.61	61.91
$^{32}S + ^{58}Ni$	1.045	9.95	60.23	9.90	60.15	9.74	60.97	9.80	60.08
$^{32}S + ^{64}Ni$	1.182	10.16	59.12	10.12	59.00	9.97	59.67	9.99	59.75
$^{34}S + ^{58}Ni$	1.090	10.06	59.65	10.02	59.53	9.88	60.18	9.90	60.20
$^{34}S + ^{64}Ni$	1.227	10.25	58.61	10.24	58.41	10.11	58.92	10.08	59.21
$^{36}S + ^{58}Ni$	1.136	10.16	59.11	10.13	58.96	10.01	59.47	10.00	59.65
$^{36}S + ^{64}Ni$	1.273	10.34	58.12	10.35	57.85	10.24	58.23	10.18	58.72
$^{34}Ar + ^{52}Ni$	0.870	9.72	69.15	9.65	69.11	9.42	70.54	9.57	69.95
$^{34}Ar + ^{54}Ni$	0.913	9.80	68.64	9.73	68.60	9.52	69.91	9.65	69.36
$^{34}Ar + ^{56}Ni$	0.956	9.88	68.15	9.81	68.11	9.61	69.32	9.73	68.34
$^{36}Ar + ^{52}Ni$	0.913	9.83	68.44	9.76	68.41	9.57	69.62	9.68	69.18
$^{36}Ar + ^{54}Ni$	0.956	9.91	67.96	9.84	67.91	9.66	69.01	9.76	68.63
$^{40}Ar + ^{58}Ni$	1.130	10.24	65.92	10.21	65.76	10.08	66.40	10.10	66.51
$^{40}Ar + ^{60}Ni$	1.174	10.31	65.54	10.29	65.34	10.17	65.92	10.16	66.14
$^{40}Ar + ^{62}Ni$	1.217	10.37	65.18	10.36	64.93	10.24	65.47	10.22	65.79
$^{40}Ar + ^{64}Ni$	1.260	10.43	64.82	10.43	64.54	10.32	65.03	10.28	65.46
$^{36}Ca + ^{50}Ni$	0.791	9.63	77.40	9.55	77.33	9.28	79.27	9.46	78.47
$^{36}Ca + ^{52}Ni$	0.833	9.72	76.78	9.64	76.73	9.39	78.51	9.56	77.72
$^{36}Ca + ^{54}Ni$	0.875	9.80	76.18	9.72	76.16	9.49	77.81	9.65	77.04
$^{36}Ca + ^{56}Ni$	0.916	9.88	75.62	9.80	75.61	9.58	77.15	9.74	76.42
$^{38}Ca + ^{52}Ni$	0.875	9.83	76.02	9.75	75.98	9.53	77.52	9.68	76.86
$^{38}Ca + ^{54}Ni$	0.916	9.91	75.46	9.83	75.42	9.63	76.83	9.77	76.23
$^{38}Ca + ^{56}Ni$	0.958	9.98	74.93	9.91	75.89	9.72	76.20	9.85	75.65
$^{40}Ca + ^{52}Ni$	0.916	9.93	75.31	9.85	75.28	9.66	76.61	9.79	76.08
$^{40}Ca + ^{54}Ni$	0.958	10.01	74.78	9.94	74.73	9.75	75.95	9.87	75.50
$^{40}Ca + ^{58}Ni$	1.042	10.15	73.80	10.10	73.70	9.93	74.74	10.02	74.45
$^{40}Ca + ^{62}Ni$	1.125	10.29	72.90	10.25	72.76	10.09	73.67	10.15	73.56
$^{40}Ti + ^{48}Ni$	0.760	9.65	84.93	9.56	84.84	9.28	87.07	9.47	86.20
$^{40}Ti + ^{50}Ni$	0.8	9.74	84.23	9.65	84.16	9.39	86.20	9.58	85.32
$^{40}Ti + ^{52}Ni$	0.84	9.82	83.56	9.74	83.51	9.50	85.38	9.68	84.52
$^{40}Ti + ^{56}Ni$	0.92	9.99	82.32	9.91	82.30	9.69	83.92	9.86	83.14
$^{42}Ti + ^{52}Ni$	0.88	9.92	82.80	9.84	82.76	9.62	84.41	9.79	83.67
$^{42}Ti + ^{56}Ni$	0.96	10.08	81.64	10.01	81.58	9.82	82.98	9.98	82.37

TABLE I. (*Continued.*)

Reaction	N/Z	R_B [a] (fm)	V_B [a] (MeV)	R_B [b] (fm)	V_B [b] (MeV)	R_B [c] (fm)	V_B [c] (MeV)	R_B [d] (fm)	V_B [d] (MeV)
$^{48}Ti + ^{58}Ni$	1.12	10.4	79.30	10.37	79.30	10.23	80.00	10.29	79.95
$^{48}Ti + ^{60}Ni$	1.16	10.47	78.84	10.45	78.84	10.31	79.43	10.35	79.49
$^{48}Ti + ^{64}Ni$	1.24	10.60	77.97	10.59	77.97	10.47	78.37	10.47	78.67
$^{46}Ti + ^{64}Ni$	1.2	10.52	78.49	10.50	78.49	10.37	79.06	10.39	79.19
$^{50}Ti + ^{60}Ni$	1.2	10.55	78.32	10.54	78.32	10.41	78.77	10.42	78.98
$^{48}Ni + ^{48}Ni$	0.714	9.72	106.92	9.63	106.69	9.30	109.78	9.59	108.54
$^{50}Ni + ^{50}Ni$	0.786	9.93	105.10	9.82	104.99	9.54	107.57	9.81	106.32
$^{52}Ni + ^{50}Ni$	0.821	10.01	104.26	9.91	104.19	9.65	106.56	9.90	105.35
$^{54}Ni + ^{50}Ni$	0.857	10.09	103.47	10.00	103.42	9.76	105.62	10.00	104.46
$^{54}Ni + ^{54}Ni$	0.928	10.26	102.00	10.18	101.91	9.97	103.76	10.17	102.81
$^{54}Ni + ^{56}Ni$	0.964	10.33	101.31	10.26	101.20	10.07	102.92	10.25	102.07
$^{56}Ni + ^{50}Ni$	0.892	10.18	102.71	10.09	102.69	9.86	104.74	10.08	103.64
$^{56}Ni + ^{52}Ni$	0.928	10.26	102.00	10.18	101.93	9.96	103.80	10.17	102.83
$^{56}Ni + ^{54}Ni$	0.964	10.33	101.31	10.26	101.20	10.07	102.92	10.25	102.07
$^{58}Ni + ^{58}Ni$	1.071	10.55	99.41	10.51	99.18	10.34	100.55	10.47	100.08
$^{58}Ni + ^{64}Ni$	1.178	10.75	97.71	10.74	97.36	10.59	98.52	10.66	98.42
$^{64}Ni + ^{64}Ni$	1.286	10.94	96.17	10.96	95.61	10.83	96.57	10.84	96.92

[a]Based on the AW 95 potential.
[b]Based on the Bass 80 potential.
[c]Based on the Denisov DP potential.
[d]Based on the Prox. 2010 potential.

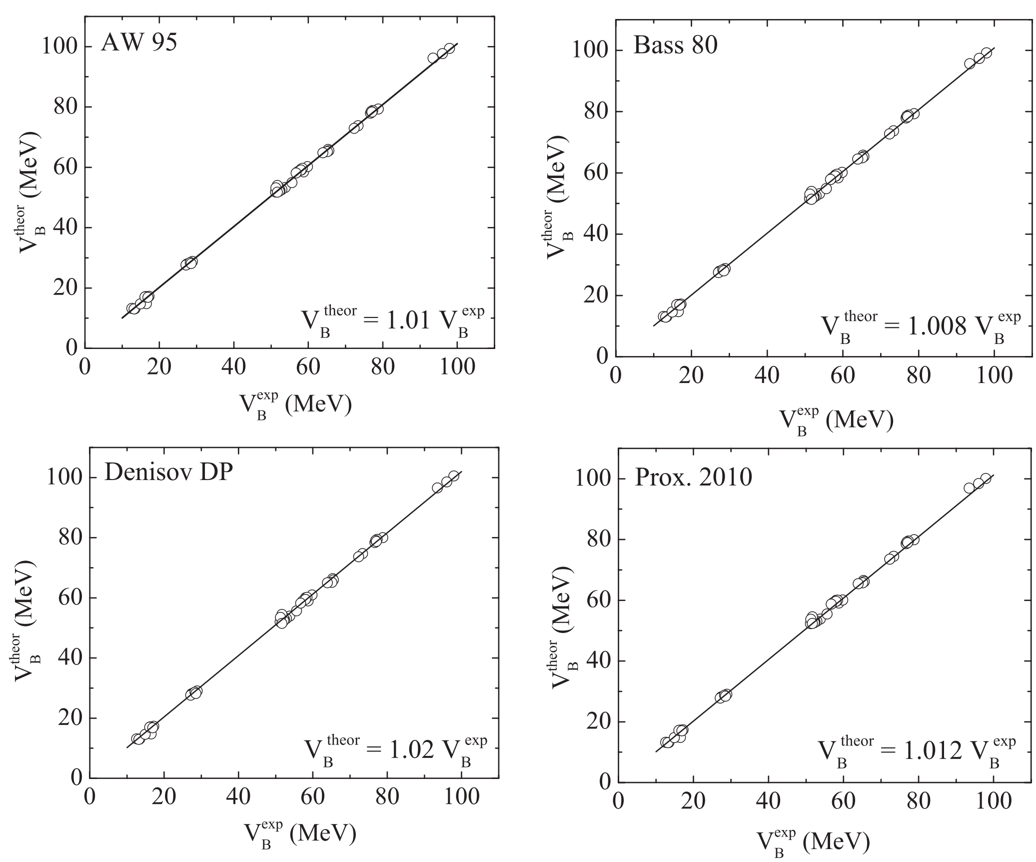

FIG. 2. The obtained theoretical barrier heights V_B^{theor} (in MeV) as a function of corresponding experimental data V_B^{exp} (in MeV) [24–40] based on the AW 95, Bass 80, Denisov DP, and Prox. 2010 potentials.

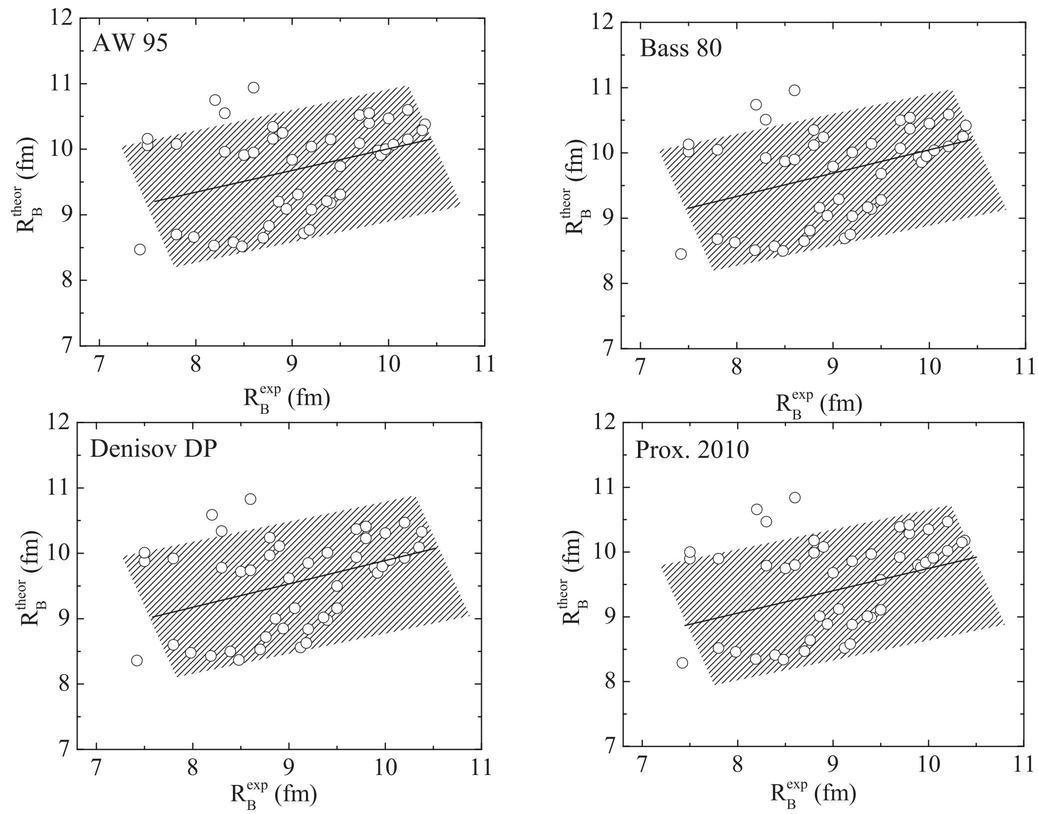

FIG. 3. The obtained theoretical barrier positions R_B^{theor} (in MeV) as a function of corresponding experimental data R_B^{exp} (in MeV) [24–40] based on the AW 95, Bass 80, Denisov DP, and Prox. 2010 potentials.

either proton- ($0.5 \leqslant N/Z \leqslant 1$) or neutron-rich ($1 \leqslant N/Z \leqslant 1.6$) systems (see Fig. 4). One can parametrize the percentage difference of R_B and V_B, which are calculated by Eqs. (14) and (15), using the below forms in the two mentioned regions, namely for $N/Z \leqslant 1$

$$\Delta R_B(\%) = \alpha_1 \left(\frac{N}{Z} - 1\right), \quad \Delta V_B(\%) = \alpha_2 \left(\frac{N}{Z} - 1\right), \tag{16}$$

and for $N/Z \geqslant 1$

$$\Delta R_B(\%) = \alpha_1' \left(\frac{N}{Z} - 1\right), \quad \Delta V_B(\%) = \alpha_2' \left(\frac{N}{Z} - 1\right), \tag{17}$$

where the values of the constants α_i and α_i', for $i = 1, 2$, are listed in Table II.

2. *Range of* $0.5 \leqslant N/Z \leqslant 1.6$

In the whole region of $0.5 \leqslant N/Z \leqslant 1.6$, the behavior of the heights and positions of the barrier are nonlinear and the percentage difference of these values can be parameterized by a second-order form (see Fig. 4)

$$\begin{aligned} \Delta R_B(\%) &= \beta_1 \left(\frac{N}{Z} - 1\right) + \beta_2 \left(\frac{N}{Z} - 1\right)^2; \\ \Delta V_B(\%) &= \beta_3 \left(\frac{N}{Z} - 1\right) + \beta_4 \left(\frac{N}{Z} - 1\right)^2, \end{aligned} \tag{18}$$

where the values of the coefficients β_i are listed in Table III. In Fig. 4, we also plotted the results of two theoretical models [3,20], for example. It is clear that the calculated values

TABLE II. The calculated values of constant coefficients α_i and α_i' that are extracted for fitting to the regular linear behavior of R_B, V_C, V_N, and V_B, Eqs. (16), (17), (20), and (21), as a function of increasing neutron in both ranges $N/Z \leqslant 1$ and $N/Z \geqslant 1$.

Proximity model	α_1	α_2	α_3	α_4	α_1'	α_2'	α_3'	α_4'
AW 95	21.24	−20.88	−23.13	51.29	16.18	−14.31	−16.06	31.45
Bass 80	21.86	−20.43	−17.14	57.68	18.26	−15.33	−23.54	41.82
Denisov DP	27.70	−27.52	−32.13	68.33	20.78	−18.11	−19.98	38.56
Prox. 2010	25.00	−24.30	−27.02	55.00	16.57	−13.63	−14.90	28.80

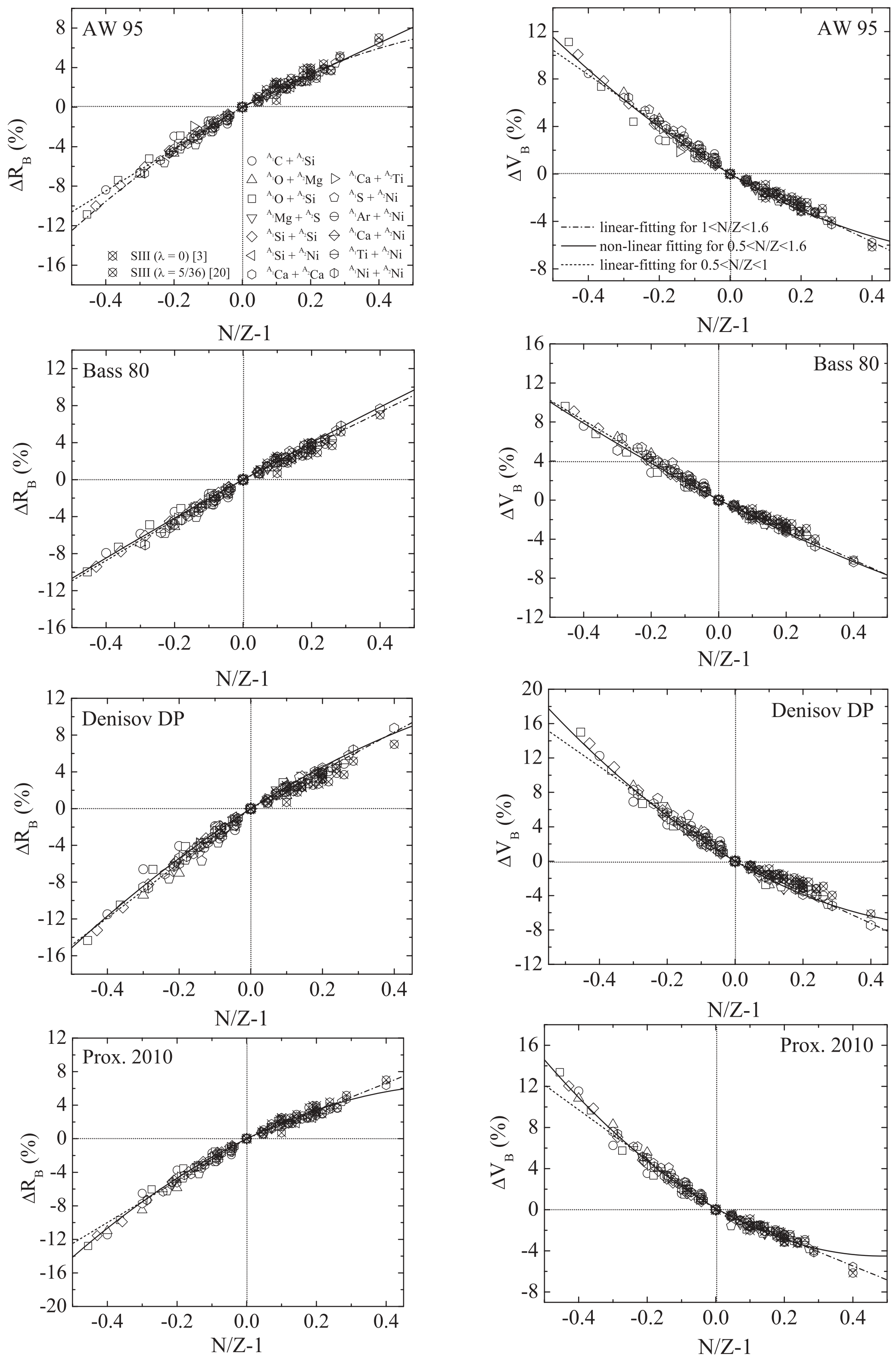

FIG. 4. The variations trend of R_B [$\Delta R_B(\%)$, left panels] and V_B [$\Delta V_B(\%)$, right panels] as a function of $(N/Z - 1)$ based on the selected potentials AW 95, Bass 80, Denisov DP, and Prox. 2010. The dashed and short-dotted lines are, respectively, used to extract the linear dependence of $\Delta R_B(\%)$ and $\Delta V_B(\%)$ values in $0.5 \leqslant N/Z \leqslant 1$ and $1 \leqslant N/Z \leqslant 1.6$ regions. The solid lines are caused by the nonlinear (second-order) fitting to the calculated values in the whole range of $0.5 \leqslant N/Z \leqslant 1.6$.

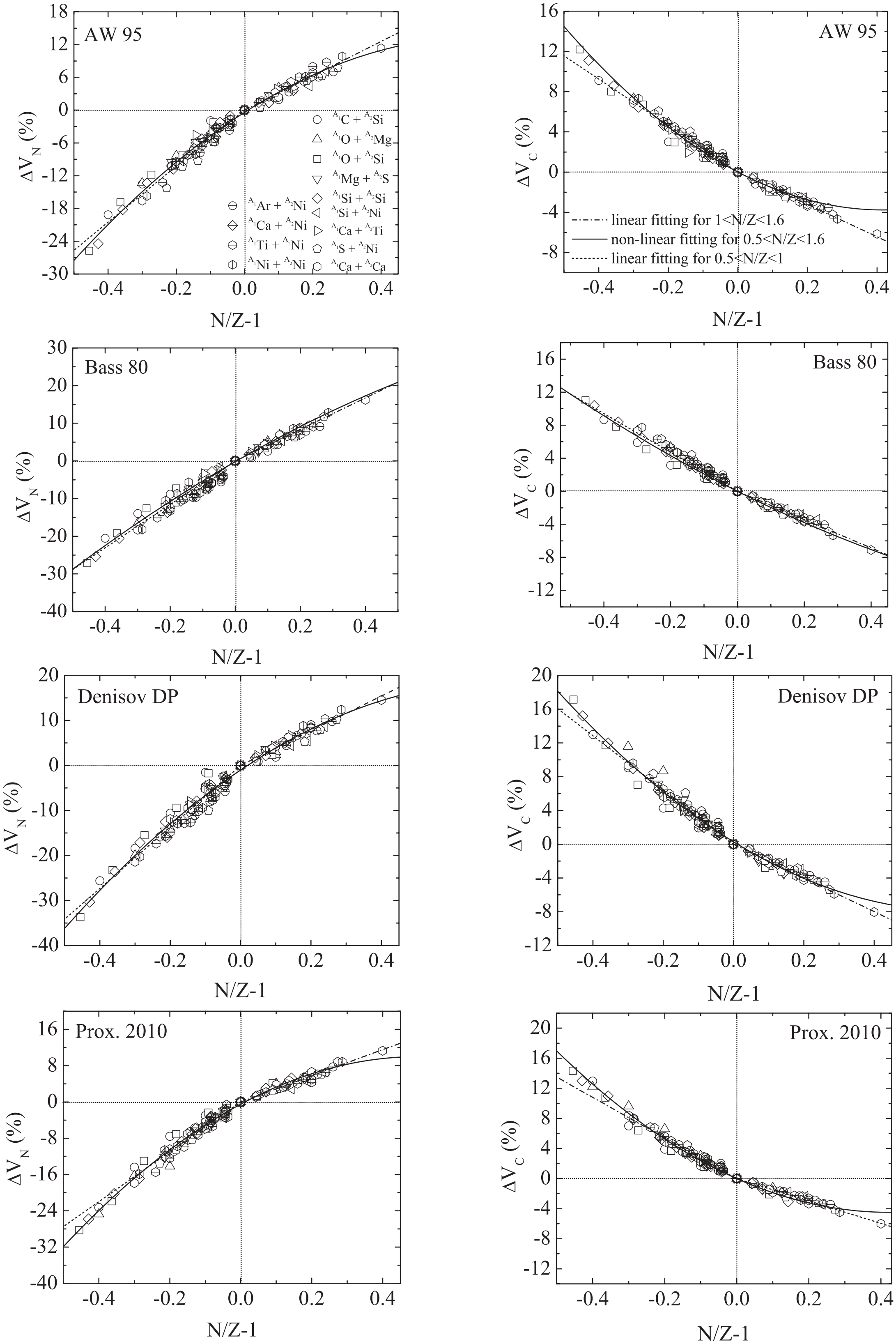

FIG. 5. The variations trend of V_N [$\Delta V_N(\%)$, left panels] and V_C [$\Delta V_C(\%)$, right panels] as a function of $(N/Z - 1)$ based on the selected potentials AW 95, Bass 80, Denisov DP, and Prox. 2010. The dashed and short-dotted lines are, respectively, used to extract the linear dependence of $\Delta R_B(\%)$ and $\Delta V_B(\%)$ values in $0.5 \leqslant N/Z \leqslant 1$ and $1 \leqslant N/Z \leqslant 1.6$ regions. The solid lines are caused by the nonlinear (second-order) fitting to the calculated values in the whole range of $0.5 \leqslant N/Z \leqslant 1.6$.

TABLE III. The calculated values of constant coefficients β_i and β_i' that are extracted for fitting to the regular nonlinear behavior of R_B, V_C, V_N, and V_B, Eqs. (18) and (23), as a function of increasing neutron in the $0.5 \leqslant N/Z \leqslant 1.6$ range.

Proximity model	β_1	β_2	β_3	β_4	β_1'	β_2'	β_3'	β_4'
AW 95	−11.25	19.38	11.03	−17.55	21.75	−18.08	−28.69	39.86
Bass 80	−1.94	20.37	4.55	−17.74	6.52	−20.26	−14.90	49.67
Denisov DP	−10.87	24.84	17.11	−22.84	20.07	−25.65	−35.30	52.69
Prox. 2010	−15.84	20.35	23.01	−19.31	26.59	−21.30	−41.85	41.88

of $\Delta R_B(\%)$ and $\Delta V_B(\%)$ for these models are consistent with our predictions. However, the results shown in Fig. 4 confirm the trend of R_B and V_B, which are reported in Refs. [2,3].

B. The isotopic dependence of nuclear V_N and Coulomb V_C potentials

In addition to R_B and V_B, we are interested in analyzing the isotopic dependence of nuclear and Coulomb potentials (at $r = R_B$) by changing neutron. For this aim, one should calculate the values of $\Delta V_N(\%)$ and $\Delta V_C(\%)$ using the following relations:

$$\Delta V_N(\%) = \frac{V_N - V_N^0}{V_N^0} \times 100, \tag{19}$$

$$\Delta V_C(\%) = \frac{V_C - V_C^0}{V_C^0} \times 100, \tag{20}$$

where V_N^0 and V_C^0 are the values of nuclear and Coulomb potentials for a symmetric reaction, see Fig. 5. Similar previous calculations of R_B and V_B and using the above suggested manner, one can predict the values of $V_N(r = R_B)$ and $V_C(r = R_B)$ for symmetric reactions that these values are not available for them. Because of the increasing neutron, it is predictable that the values of the nuclear and Coulomb potentials for different isotopic systems increase and decrease, respectively. The regular behaviors of V_N and V_C at $r = R_B$ are examined in the following ranges.

1. Ranges of $0.5 \leqslant N/Z \leqslant 1$ *and* $1 \leqslant N/Z \leqslant 1.6$

The values of Coulomb and nuclear potentials based on the AW 95, Bass 80, Denisov DP, and Prox. 2010 potentials follow a linear dependence for either proton- ($0.5 \leqslant N/Z \leqslant 1$) or neutron-rich ($1 \leqslant N/Z \leqslant 1.6$) systems (see Fig. 5). The

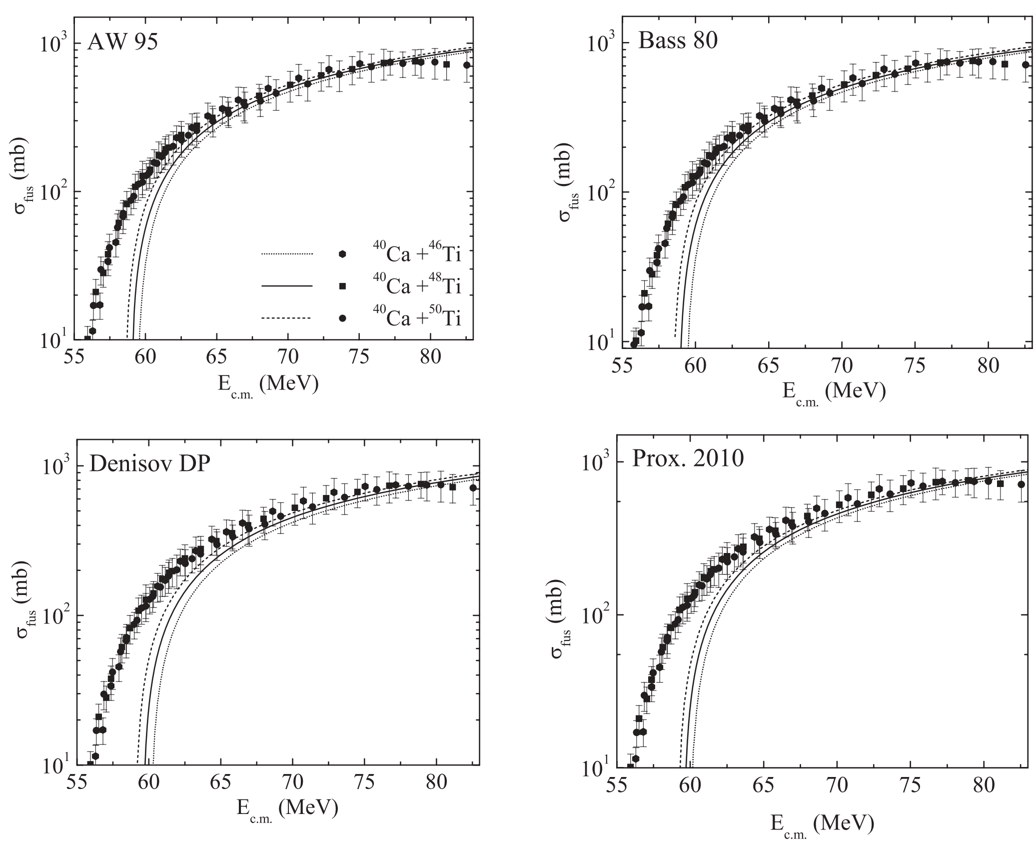

FIG. 6. The comparison of theoretical, Eq. (25), and experimental data [23] for fusion cross sections based on the various versions of proximity formalism, namely AW 95, Bass 80, Denisov DP, and Prox. 2010 potentials. These calculations have been carried out for ^{40}Ca + ^{46}Ti, ^{40}Ca + ^{48}Ti, and ^{40}Ca + ^{50}Ti fusion reactions.

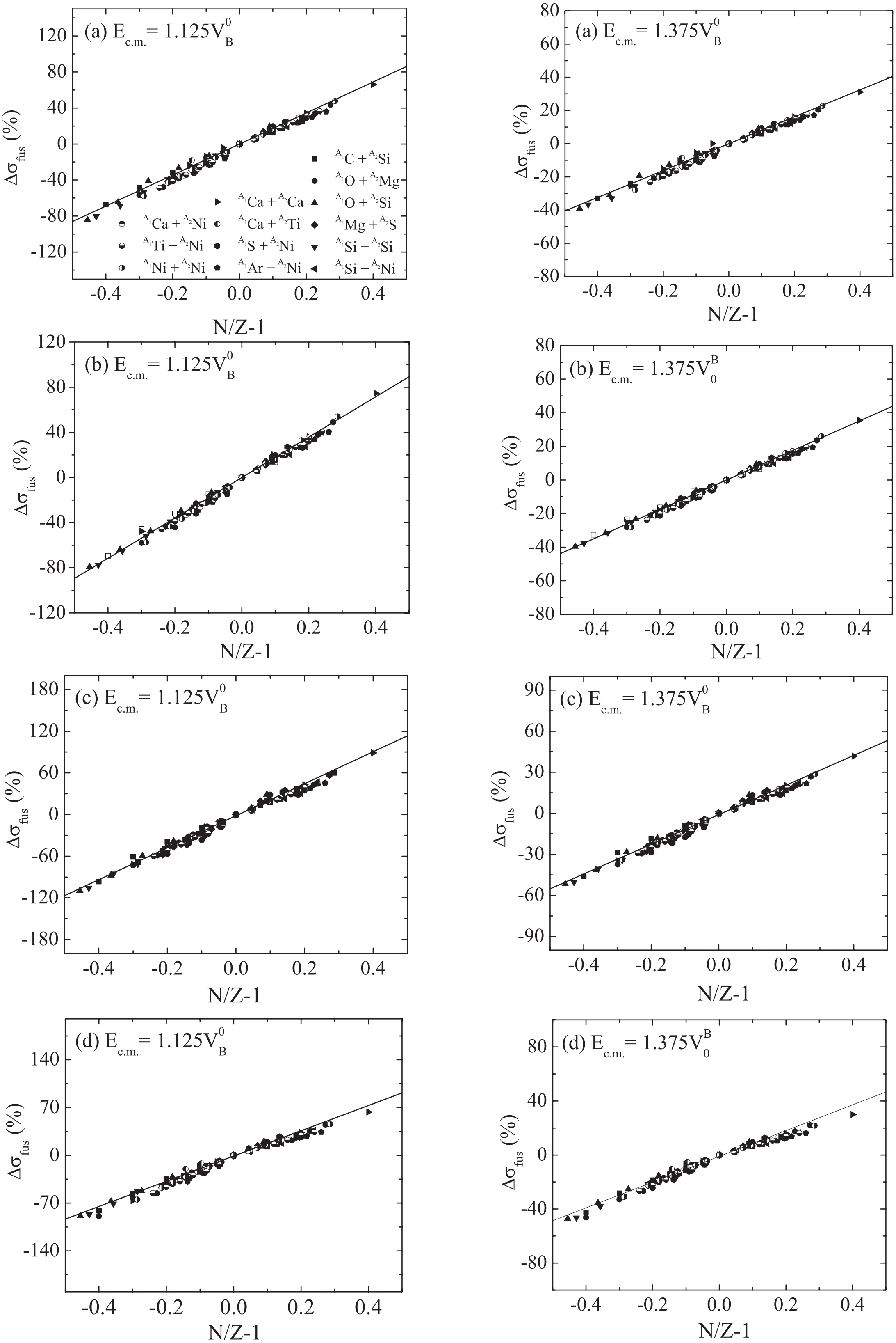

FIG. 7. The percentage difference of fusion cross sections $\Delta\sigma_{\rm fus}(\%)$ as a function of $(N/Z-1)$ for different colliding systems. These values are calculated for two instances of the above barrier energies, namely $E_{\rm c.m.} = 1.125V_B^0$ (left panels) and $E_{\rm c.m.} = 1.375V_B^0$ (right panels), which are based on the (a) AW 95, (b) Bass 80, (c) Denisov DP, and (d) Prox. 2010 potentials. The linear behavior of $\sigma_{\rm fus}$ has been parameterized by solid lines [Eq. (27)].

percentage differences of V_C and V_N are parameterized as the following forms for $N/Z \leqslant 1$:

$$\Delta V_C(\%) = \alpha_3 \left(\frac{N}{Z} - 1\right), \quad \Delta V_N(\%) = \alpha_4 \left(\frac{N}{Z} - 1\right), \tag{21}$$

and for $N/Z \geqslant 1$

$$\Delta V_C(\%) = \alpha_3' \left(\frac{N}{Z} - 1\right); \quad \Delta V_N(\%) = \alpha_4' \left(\frac{N}{Z} - 1\right), \tag{22}$$

where the values of constants α_i and α_i', for $i = 3, 4$, are listed in Table II.

2. *Range of* $0.5 \leqslant N/Z \leqslant 1.6$

In the range of $0.5 \leqslant N/Z \leqslant 1.6$, we found a nonlinear regular behavior for both nuclear and Coulomb potentials. One can formulate these trends as

$$\begin{aligned} \Delta V_C(\%) &= \beta_1' \left(\frac{N}{Z} - 1\right) + \beta_2' \left(\frac{N}{Z} - 1\right)^2; \\ \Delta V_N(\%) &= \beta_3' \left(\frac{N}{Z} - 1\right) + \beta_4' \left(\frac{N}{Z} - 1\right)^2, \end{aligned} \tag{23}$$

where the values of coefficients β_i' are listed in Table III.

IV. ISOTOPIC ANALYSIS OF FUSION CROSS SECTIONS

In the present study, the one-dimensional penetration model [21,22] is used to study the fusion cross section σ_{fus}. In this formalism, the σ_{fus} is defined as the summation on the quantum-mechanical transmission probability through the potential barrier for a specified angular momentum l and center-of-mass energy, namely $T_l(E_{\text{c.m.}})$

$$\sigma_{\text{fus}} = \frac{\pi\hbar^2}{2\mu E_{\text{c.m.}}} \sum_{l=0}^{l_{\max}} (2l+1) T_l(E_{\text{c.m.}}), \tag{24}$$

where in this relation μ is the reduced mass of the interacting system. With the assumption that $E_{\text{c.m.}} \gg V_B$, Eq. (24) reduces to the well-known sharp cutoff formula

$$\sigma_{\text{fus}} = 10\pi R_B^2 \left(1 - \frac{V_B}{E_{\text{c.m.}}}\right). \tag{25}$$

Among the introduced potentials in Refs. [10–12], we selected the models that have the best agreement with fusion data. To get a better comparison, the fusion cross sections for the ^{A_1}Ca + ^{A_2}Ti system, namely ^{40}Ca + ^{46}Ti, ^{40}Ca + ^{48}Ti, and ^{40}Ca + ^{50}Ti fusion reactions, are calculated by the sharp cutoff formula, Eq. (25). For this purpose, we used the obtained results of R_B and V_B based on the AW 95, Bass 80, Denisov DP, and Prox. 2010 potentials (see Fig. 6). In this figure, the corresponding experimental data for considered reactions are taken from Ref. [23]. It is shown that the predicted values for fusion cross sections are consistent with the experimental data particularly at the above barrier energies.

TABLE IV. The calculated values of constant coefficients γ that are extracted for fitting to the regular linear behavior of σ_{fus}, Eq. (27), as a function of $N/Z - 1$.

Proximity model	γ (for $E_{\text{c.m.}} = 1.125V_B^0$)	γ (for $E_{\text{c.m.}} = 1.375V_B^0$)
AW 95	172.21	80.94
Bass 80	178.82	87.60
Denisov DP	22.31	108.35
Prox. 2010	185.03	95.28

To the systematic study of fusion cross section in isotopic systems we have defined the percentage difference of this quantity, namely $\Delta\sigma_{\text{fus}}(\%)$, as the following form:

$$\Delta\sigma_{\text{fus}}(\%) = \frac{\sigma_{\text{fus}}(E_{\text{c.m.}}^0) - \sigma_{\text{fus}}^0(E_{\text{c.m.}}^0)}{\sigma_{\text{fus}}^0(E_{\text{c.m.}}^0)} \times 100, \tag{26}$$

where the $\sigma_{\text{fus}}(E_{\text{c.m.}}^0)$ is the fusion cross section for a reaction with the $N = Z$ condition. We computed the $\Delta\sigma_{\text{fus}}(\%)$ at some above barrier energies such as $E_{\text{c.m.}} = 1.125V_B^0$ and $E_{\text{c.m.}} = 1.375V_B^0$. The calculated results are shown in Fig. 7. It is clear that by increasing the neutron in interacting systems and decreasing the barrier height, one expects that fusion cross sections enhance. This behavior is quite obvious in Fig. 7. In contrast, the obtained results for barrier characteristics, the relationship between variations of fusion cross sections $\Delta\sigma_{\text{fus}}(\%)$, and the increasing of $(N/Z - 1)$ quantity is linear. This subject is accurate for all neutron- and proton-rich systems ($0.5 \leqslant N/Z \leqslant 1.6$). We parameterized this linear trend of fusion cross sections as the following form:

$$\Delta\sigma_{\text{fus}}(\%) = \gamma \left(\frac{N}{Z} - 1\right), \tag{27}$$

where the values of constant coefficient γ have been listed in Table IV for various potentials and energies.

V. CONCLUSION

In this paper, using the systematic study on the large range of colliding pairs C, O, Mg, Si, S, S, Ca, Ar, Ti, and Ni with $84 \leqslant Z_1Z_2 \leqslant 784$, we analyzed the isotopic dependence of different parameters of interacting potentials and fusion cross sections. For calculating these values, we used four confirmed versions of the proximity formalism and Wong model. Our obtained results for the three considered regions of the N/Z ratio (i.e., $0.5 \leqslant N/Z \leqslant 1$, $1 \leqslant N/Z \leqslant 1.6$, and $0.5 \leqslant N/Z \leqslant 1.6$) are as follows. (a) For fusion systems with the condition of $0.5 \leqslant N/Z \leqslant 1$, the variations trend of barrier characteristics, R_B, $V_C(R = R_B)$, $V_N(R = R_B)$, and V_B, with respect to the corresponding symmetric reaction ($N = Z$), follow a linear dependence as a function of $(N/Z - 1)$. (b) For colliding systems with a condition of $1 \leqslant N/Z \leqslant 1.6$, the above quantities can be parameterized as linear. (c) In the whole range $0.5 \leqslant N/Z \leqslant 1.6$, the values of ΔR_B, ΔV_C, ΔV_N, and ΔV_B have different trends. In other words, these values follow a nonlinear second-order behavior with the addition/removal of the neutron.

As a common property, one can point out the values of R_B, $V_N(R = R_B)$ as well as V_B, $V_C(R = R_B)$, respectively, increase and decrease with the increasing of the neutron. However, the fusion cross sections follow a linear dependence for all considered isotopic systems.

[1] R. K. Puri, M. K. Sharma, and R. K. Gupta, Eur. Phys. J. A **3**, 277 (1998).
[2] R. K. Puri and N. K. Dhiman, Eur. Phys. J. A **23**, 429 (2005).
[3] N. K. Dhiman and R. K. Puri, Acta. Phys. Pol. B **37**, 1855 (2006).
[4] K. Siwek-Wilczynska, I. Skwira-Chalot, and J. Wilczynski, Int. J. Mod. Phys. E **16**, 483 (2007).
[5] O. N. Ghodsi and R. Gharaei, Eur. Phys. J. A **48**, 21 (2012).
[6] A. Winther, Nucl. Phys. A **594**, 203 (1995).
[7] R. Bass, Phys. Rev. Lett. **39**, 265 (1977).
[8] R. Bass, in *Lecture Notes in Physics*, Vol. 117 (Springer, Berlin, 1980), pp. 281–293.
[9] V. Y. Denisov, Phys. Lett. B **526**, 315 (2002).
[10] I. Dutt and R. K. Puri, Phys. Rev. C **81**, 047601 (2010).
[11] I. Dutt and R. K. Puri, Phys. Rev. C **81**, 064609 (2010).
[12] I. Dutt and R. K. Puri, Phys. Rev. C **81**, 044615 (2010).
[13] C. Y. Wong, Phys. Lett. B **42**, 186 (1972); Phys. Rev. Lett. **31**, 766 (1973).
[14] S. Gautam, A. D. Sood, R. K. Puri, and J. Aichelin, Phys. Rev. C **83**, 034606 (2011).
[15] S. Gautam, A. D. Sood, R. K. Puri, and J. Aichelin, Phys. Rev. C **83**, 014603 (2011).
[16] S. Goyal and R. K. Puri, Nucl. Phys. A **853**, 164 (2011).
[17] S. Gautam, R. Chugh, A. D. Sood, R. K. Puri, Ch. Hartnack, and J. Aichelin, J. Phys. G **37**, 085102 (2010).
[18] N. Wang, Z. Li, and X. Wu, Phys. Rev. C **65**, 064608 (2002).
[19] J. Blocki, J. Randrup, W. J. Swiatecki, and C. F. Tsang, Ann. Phys. (NY) **105**, 427 (1977).
[20] R. K. Puri and R. K. Gupta, Phys. Rev. C **45**, 1837 (1992).
[21] S. G. Steadman and M. J. Rhoades-Brown, Annu. Rev. Nucl. Sci. **36**, 649 (1986).
[22] M. Beckerman, Rep. Prog. Phys. **51**, 1047 (1988).
[23] A. A. Sonzogni, J. D. Bierman, M. P. Kelly, J. P. Lestone, J. F. Liang, and R. Vandenbosch, Phys. Rev. C **57**, 722 (1998).
[24] S. Gary and C. Volant, Phys. Rev. C **25**, 1877 (1982).
[25] L. C. Vaz, J. M. Alexander, and G. R. Satchler, Phys. Rep. **69**, 373 (1981).
[26] C. M. Jachcinski, D. G. Kovar, R. R. Betts, C. N. Davids, D. F. Geesaman, C. Olmer, M. Paul, S. J. Sanders, and J. L. Yntema, Phys. Rev. C **24**, 2070 (1981).
[27] R. Rascher, W. F. J. Müller, and K. P. Lieb, Phys. Rev. C **20**, 1028 (1979).
[28] D. G. Kovar, D. F. Geesaman, T. H. Braid, Y. Eisen, W. Henning, T. R. Ophel, M. Paul, K. E. Rehm, S. J. Sanders, P. Sperr, J. P. Schiffer, S. L. Tabor, S. Vigdor, B. Zeidman, and F. W. Prosser, Phys. Rev. C **20**, 1305 (1979).
[29] G. M. Berkowitz, P. Braun-Munzinger, J. S. Karp, R. H. Freifelder, T. R. Renner, and H. W. Wilschut, Phys. Rev. C **28**, 667 (1983).
[30] E. F. Aguilera, J. J. Kolata, P. A. DeYoung, and J. J. Vega, Phys. Rev. C **33**, 1961 (1986).
[31] A. M. Stefanini, G. Fortuna, R. Pengo, W. Meczynski, G. Montagnoli, L. Corradi, A. Tivelli, S. Beghini, C. Signorini, S. Lunardi, M. Morando, and F. Soramel, Nucl. Phys. A **456**, 509 (1986).
[32] H. A. Aljuwair, R. J. Ledoux, M. Beckerman, S. B. Gazes, J. Wiggins, E. R. Cosman, R. R. Betts, S. Saini, and O. Hansen, Phys. Rev. C **30**, 1223 (1984).
[33] E. Tomasi, D. Ardouin, J. Barreto, V. Bernard, B. Cauvin, C. Magnago, C. Mazur, C. Ngo, E. Piasecki, and M. Ribrag, Nucl. Phys. A **373**, 341 (1982).
[34] M. Trotta, A. M. Stefanini, L. Corradi, A. Gadea, F. Scarlassara, S. Beghini, and G. Montagnoli, Phys. Rev. C **65**, 011601(R) (2001).
[35] A. A. Sonzogni, J. D. Bierman, M. P. Kelly, J. P. Lestone, J. F. Liang, and R. Vandenbosch, Phys. Rev. C **57**, 722 (1998).
[36] Q. Haider and F. B. Malik, Phys. Rev. C **26**, 162 (1982).
[37] U. Jahnke, H. H. Rossner, D. Hilscher, and E. Holub, Phys. Rev. Lett. **48**, 17 (1982).
[38] A. M. Vinodkumar, K. M. Varier, N. V. S. V. Prasad, D. L. Sastry, A. K. Sinha, N. Madhavan, P. Sugathan, D. O. Kataria, and J. J. Das, Phys. Rev. C **53**, 803 (1996).
[39] N. V. S. V. Prasadet, A. M. Vinodkumar, A. K. Sinha, K. M. Varier, D. L. Sastry, N. Madhavan, P. Sugathan, D. O. Kataria, J. J. Das *et al.*, Nucl. Phys. A **603**, 176 (1996).
[40] M. Beckerman, M. Salomaa, A. Sperduto, J. D. Molitoris, and A. DiRienzo, Phys. Rev. C **25**, 837 (1982).